Eur. Phys. J. E (2015) **38**: 101
DOI 10.1140/epje/i2015-15101-9

THE EUROPEAN PHYSICAL JOURNAL E

Regular Article

Counterion-mediated protein adsorption into polyelectrolyte brushes

Su-zhen He[1,2,a], Holger Merlitz[2,3], Jens-Uwe Sommer[3], and Chen-Xu Wu[2]

[1] School of Mechanical and Electrical Engineering, Putian University, Putian 351100, P.R. China
[2] Department of Physics and ITPA, Xiamen University, Xiamen 361005, P.R. China
[3] Leibniz-Institut für Polymerforschung Dresden, 01069 Dresden, Germany

Received 25 May 2015 and Received in final form 6 August 2015
Published online: 21 September 2015 –

Abstract. We present molecular dynamics simulations of the interaction of fullerene-like, inhomogeneously charged proteins with polyelectrolyte brushes. A motivation of this work is the experimental observation that proteins, carrying an integral charge, may enter like-charged polymer brushes. Simulations of varying charge distributions on the protein surfaces are performed to unravel the physical mechanism of the adsorption. Our results prove that an overall neutral protein can be strongly driven into polyelectrolyte brush whenever the protein features patches of positive and negative charge. The findings reported here give further evidence that the strong adsorption of proteins is also driven by entropic forces due to counterion release, since charged patches on the surface of the proteins can act as multivalent counterions of the oppositely charged polyelectrolyte chains. A corresponding number of mobile co- and counterions is released from the brush and the vicinity of the proteins so that the entropy of the total system increases.

1 Introduction

The study of interactions of proteins with solid surfaces is an important field of biotechnology [1]. In many biomedical applications, an adsorption of proteins has to be prevented. Polymer brushes, coated onto substrates, have been shown to feature such "anti-fouling" properties because they sterically prevent proteins from approaching the substrates [2, 3]. On the other hand, polyelectrolyte brushes are capable of adsorbing proteins if the ionic strength in the system is low [4], and the addition of salt leads to a subsequent release of these proteins. More complex brushes made of mixed polymers have been used to reversibly adsorb and release proteins, depending on the environmental conditions, and may therefore serve as drug delivery systems [5, 6].

An interesting phenomenon is the adsorption of charged proteins into brushes made of polymers of identical charge, sometimes named "adsorption on the wrong side" [4,6–9]. Here, a driving force has to exist that allows the proteins to overcome both the osmotic pressure of the brush and the electrostatic repulsion between protein and polymer. One potential mechanism to drive the proteins into the brush is based on a charge regulation/reversal upon the approach of the protein in weakly charged systems [7, 10]. By adjusting the pH in the brush layer at a low ionic strength, the pI of protein is higher than the pH within the brush layer. Hence the net charge of protein is reversed and a strong unlike-charge electrostatic attraction arises. This model successfully revealed that pH is an important parameter in polyelectrolyte-mediated protein adsorption (PMPA), but fails to explain the experimental observation of strong protein adsorption at pH values exceeding the pI [4]. This would indicate that the pH is an important, but not exclusive or even decisive parameter. An alternative argumentation has been proposed in which counterion release plays the central role for adsorption on the wrong side [4, 9, 11, 12]. As an example, negatively charged polyelectrolyte chains can interact with the positive charges on the surface of the protein molecules, during which that protein patch acts like a multivalent counterion which replaces several monovalent counterions of polyelectrolyte chains. The respective counterions of the proteins, together with the positive counterions of the chains, are released. The release of ions causes an entropy-driven gain in free energy which results into an attractive contribution to the effective interaction between the polyelectrolyte and the protein [13]. Protein adsorption can be performed to test the behavior of the mixed polyelectrolyte brushes in contact with biosystems [6, 14]. The high-performance smart substrates created by mixed brushes could be applied in domains as diverse as biosensors, drug delivery and nanotransport [14].

[a] e-mail: hesuzan@126.com

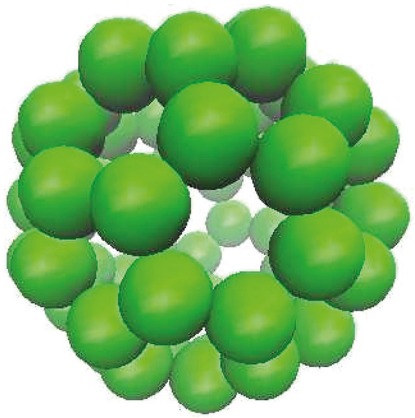

Fig. 1. Scheme of C60 fullerene-like protein.

2 Simulation methodology

A coarse-grained model was used to investigate the adsorption of neutral and nonuniformly charged proteins on planar PEBs in salt-free and salt-added solution. The polyelectrolyte chains were created as a coarse-grained bead-spring model with negatively charged bead, anchored at one end to an uncharged planar surface to form a regular 8×8 square grid. A moderate grafting density $\sigma = 0.05d^{-2}$, where d is monomer size. The charged chains were monodisperse, with the degree of polymerizations $N = 40$ and the charge fraction was parameterized by $f = 1$. The same number of oppositely charged counterions were added to keep electroneutrality. To model charged proteins, we utilized the fullerene C60 structure by rescaling the coordinates of the C atoms in such a way to set the diameter to 17.4 Å (see fig. 1). We choose some of the 60 beads to be charged negatively or positively according to what kind of patten we need. The same number of cations and anions were added. The protein is treated as a rigid body where hydrogen bonds are neglected. The solvent is assumed to be athermal which induced hydrophobic interactions here. The excluded-volume interactions are introduced via a pure short-ranged repulsive LJ potential, given by

$$U_{\mathrm{LJ}}(r) = 4\epsilon \left[\left(\frac{d}{r}\right)^{12} - \left(\frac{d}{r}\right)^{6} - \left(\frac{d}{r_c}\right)^{12} + \left(\frac{d}{r_c}\right)^{6} \right]. \tag{1}$$

The cutoff radius was $r_c = 2^{1/6}d$, d being the size of the bead and ϵ the potential depth.

Beads along the polymer chains were coupled by a FENE (finitely extensible nonlinear elastic) bond potential [15]

$$U_{\mathrm{FENE}} = -0.5KR^2 \ln\left[1 - \left(\frac{r}{R}\right)^2\right] + 4\epsilon\left[\left(\frac{d}{r}\right)^{12} - \left(\frac{d}{r}\right)^{6}\right] + \epsilon, \tag{2}$$

with spring constant $k = 30\epsilon/d^2$ and maximum bond length $R = 1.5d$.

The wall was modeled as a 9-3 LJ potential

$$U_{\mathrm{wall}} = \epsilon\left[\frac{2}{15}\left(\frac{d}{r}\right)^9 - \left(\frac{d}{r}\right)^3\right], \tag{3}$$

with d being the particle size. One wall was located at $z = 0$, the same height as the substrate to which the chains were grafted. The Coulomb interaction was of long range and had to be addressed with particular care. The simulation package LAMMPS includes the implementation of the particle-particle/particle-mesh (PPPM) algorithm [16–18] that solves the field equation on a lattice through fast Fourier transformation. In this way, the influence of periodic images of charged particles (that show up in both horizontal x- and y-directions) were properly accounted for. Formally, the Coulomb potential is written as

$$U_{\mathrm{Coul}}(r) = l_B k_B T \sum_{n_x=-\infty}^{\infty} \sum_{n_y=-\infty}^{\infty} \sum_{i=1}^{N_{\mathrm{tot}}-1} \sum_{j=i-1}^{N_{\mathrm{tot}}} \frac{q_i q_j}{|\mathbf{r}_{ij} + n_x L\mathbf{e}_x + n_y L\mathbf{e}_y|}, \tag{4}$$

where q_i and q_j are the corresponding charges and $l_B = e^2/(4\pi\varepsilon_0\varepsilon k_B T)$ the Bjerrum length, that defines the distance at which both Coulomb energy and thermal energy ($k_B T$) are of the same magnitude. $\mathbf{e}_x$ and $\mathbf{e}_y$ are unit vectors in x-y direction, and the indices n_x and n_y run over the periodic images of the simulation box. N_{tot} is the total number of charges and L the box-size in xy-directions.

The total interaction potential was composed of four contributions:

$$U_{\mathrm{tot}} = U_{\mathrm{FENE}} + U_{\mathrm{LJ}} + U_{\mathrm{wall}} + U_{\mathrm{Coul}}. \tag{5}$$

The equation of motion was defined as a Langevin equation:

$$m\frac{\mathrm{d}^2\mathbf{r}_i}{\mathrm{d}t^2} + \varsigma\frac{\mathrm{d}\mathbf{r}_i}{\mathrm{d}t} = -\frac{\partial U_{\mathrm{tot}}}{\partial \mathbf{r}_i} + \mathbf{F}_i, \tag{6}$$

where m is the particle mass and ς the friction constant. $\mathbf{F}_i$ is a Gaussian random force that was used to couple the system to the heat bath, with the correlation function

$$\langle \mathbf{F}_i(t) \cdot \mathbf{F}_j(t')\rangle = 6mk_B T\varsigma\delta_{ij}\delta(t - t'). \tag{7}$$

The temperature was $k_B T = 0.6\epsilon$, and the damping constant $\varsigma = 0.5\tau_{\mathrm{LJ}}^{-1}$, with $\tau_{\mathrm{LJ}} = (md^2/\epsilon)^{1/2}$ being the Lennard-Jones time. Each simulation contains 8×10^7 steps for equilibration of system, and the following 8×10^6 steps for the ensemble average.

3 Polyelectrolyte-mediated protein adsorption: Survey of simulation results

Protein adsorption on flat and fixed surfaces is relatively easy to analyze. This simultion paper analyses the question whether a counterion release mechanism is sufficiently

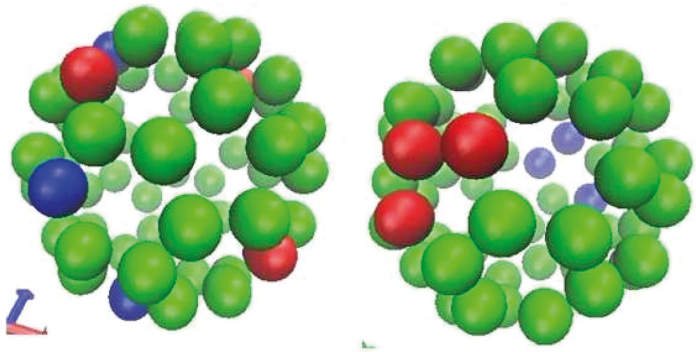

Fig. 2. Charge distributions on the fullerene-like protein models: (a) Randomly charged beads, yielding a negligible dipole moment. (b) Positive and negative surface patches with a considerable dipole moment. Both proteins are electroneutral.

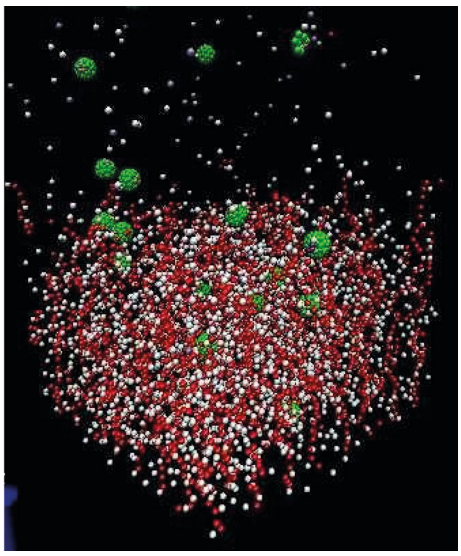

Fig. 3. Snapshot of a polymer brush (red) with partially adsorbed proteins (green). Mobile counterions are white.

effective to grant the protein adsorption of condensation is possible. While there is clear experimental evidence for the PMPA, a corresponding computer simulation is still lacking. Here, we perform molecular dynamics simulations of coarse-grained protein and brush models to study PMPA. The adsorption behavior is separately investigated under conditions of proteins which are neutral, of vanishing total charge but with oppositely charged patches, as well as proteins with a nonvanishing net charge, aiming at finding the condition in which the proteins begin to adsorb. Figure 3 displays a snapshot of a typical system after equilibration.

The protein is modeled as a fullerene-like sphere made of coarse-grained beads, as shown in fig. 2. The distributions of charges vary: Figure 2(a) shows a randomly distributed charge pattern which yields a negligible total dipole moment of the molecule, while in the case of fig. 2(b), the opposite charges are forming clusters or patches. Since these patches occupy opposite poles on the molecule, they lead to a significant dipole moment. Details about the protein models are summarized in table 1.

Density distributions of monomers and proteins after an equilibration of each system are shown in fig. 4. The protein model corresponding to each subgraph is presented in table 1.

We shall first focus on fig. 4(a) and (e): the amount of adsorbed proteins in fig. 4(a) is nearly five times as high as in fig. 4(e). The electroneutral proteins of the system simulated in fig. 4(a) has two domains (see fig. 2(b)), one with positive charges and the other one with negative charges, which together form an electric dipole. In fig. 4(e), the proteins have zero net charges as well, but the charges are randomly distributed (see fig. 2(a)), corresponding to a multipolar charge distribution.

The major difference between both protein types lies in the counterion condensation that occurs with the free (non-adsorbed) protein, when the charges on its surface form well-defined and separated patches with locally high charge densities. Figure 7 shows the protein-counterion correlation functions of both protein models, for the case of free proteins: The charged patches allow for a counterion localization which reduces the entropy of the involved counterions (black squares). If the charges on the protein surface are randomly distributed, the electrostatic interaction is insufficient to localize the counterions, which thus remain delocalized in the solvent.

Once a protein with its counterion cloud is inserted into the brush, negatively charged monomers are getting attached to the positive patches of the proteins. As a result, the counterions of both the protein patch as well as those from the PEBs are released. This process is entropically favorable, because the released counterions become fully delocalized and hence they reduce the free energy of the system by an amount of the order of k_BT per counterion.

Figure 4(d) and (c) indicate that the driving force generated by the counterion release is effective even when the proteins are overall negatively charged, which is the same charge as the monomers. Once again, more proteins are adsorbed if they feature charged surface patches, fig. 4(d), compared to the alternative model in which the

Table 1. Protein configurations.

Parameters \ Sequence number	fig. 4a fig. 2b	fig. 4b	fig. 4c	fig. 4d	fig. 4e fig. 2a	fig. 4f
Number of positive charges	3	0	3	3	3	3
Number of negative charges	3	0	4	4	3	3
Total charge	0	0	−1	−1	0	0
Charge distribution	patch		random	patch	random	patch

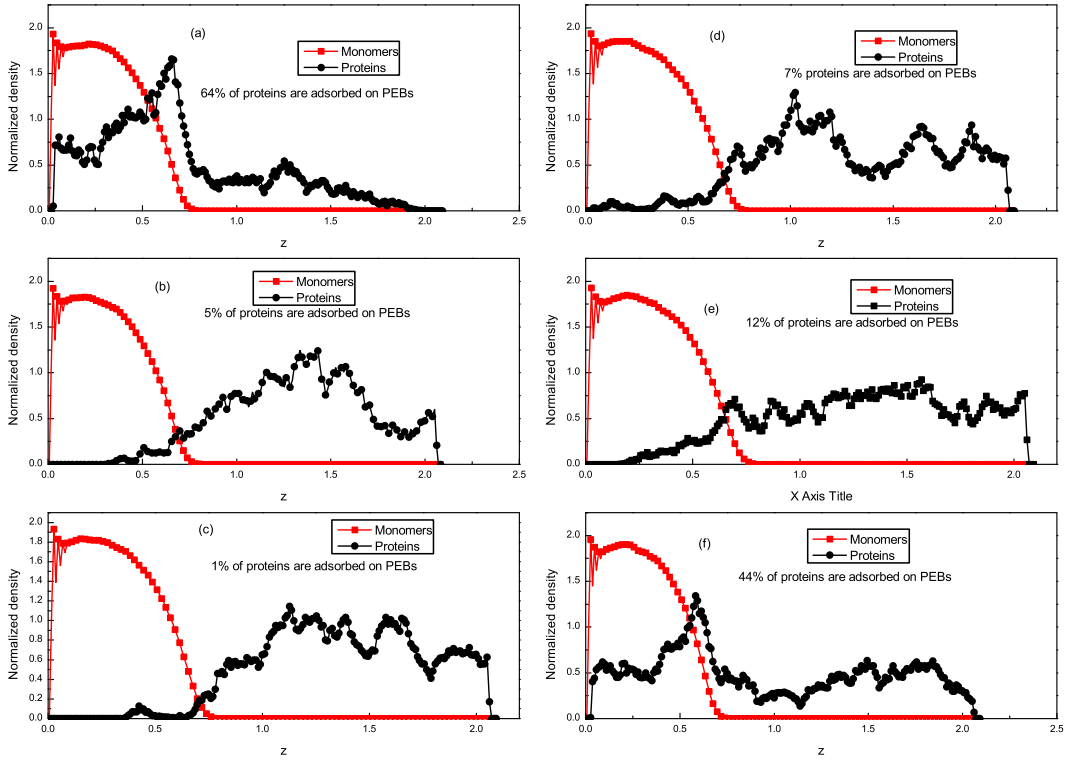

Fig. 4. Normalized vertical density distributions of proteins (black) and brush-monomers (red). The proteins are: (a) electroneutral with positive and negative surface patches; (b) neutral; (c) negatively charged, with randomly distributed charges; (d) negatively charged, with positive and negative surface patches; (e) electroneutral, with randomly distributed charges; (f) like (a), but in salt solution, $C_s = 0.03\,\mathrm{M/L}$.

charges are distributed randomly, fig. 4(c). For a comparison, fig. 4(b) displays the situation of fully neutral proteins in the absence of any charges. Due to the steric repulsion caused by the compression of stretched chains, protein adsorption is strongly suppressed in this case. Note the comparison with the system shown in fig. 4(d), in which the adsorption which is enthalpically less favorable, yet somewhat more pronounced as a result of the charged patches and the corresponding counterion release.

In order to approach a quantitative understanding of the counterion release, we are now going to count the average numbers of counterions in the vicinity of the proteins, before and after protein adsorption(fig. 5 and fig. 6).

To define the coordination number, we have calculated the radial distribution $g(r)$. The positions, labeled by dotted line in fig. 5, which separates the first and the second peak are thus assumed to comprise the first nearest neighborhood of given protein. Therefore, the number of neighbors of each protein within this position determines the coordination number. From fig. 5(a), it was found that each protein with two surface patches is surrounded by 5 counterions before adsorption. Figure 6(a) indicates that some counterions of proteins are released and proteins replace the counterions of polyelectrolyte chains after adsorption, that the neighbor number for counterion drops to 2 and that the neighbor number for monomers is about 2. For the model that charges are randomly distributed on protein surface, we observed that the pair correlation function profile did not show the obvious gap due to low charge density. Before adsorption, proteins only can hold about 2 counterions surrounded them (see fig. 5(b)). After adsorption, these two counterions are released and replaced by 2 monomers which can be found in fig. 6(b).

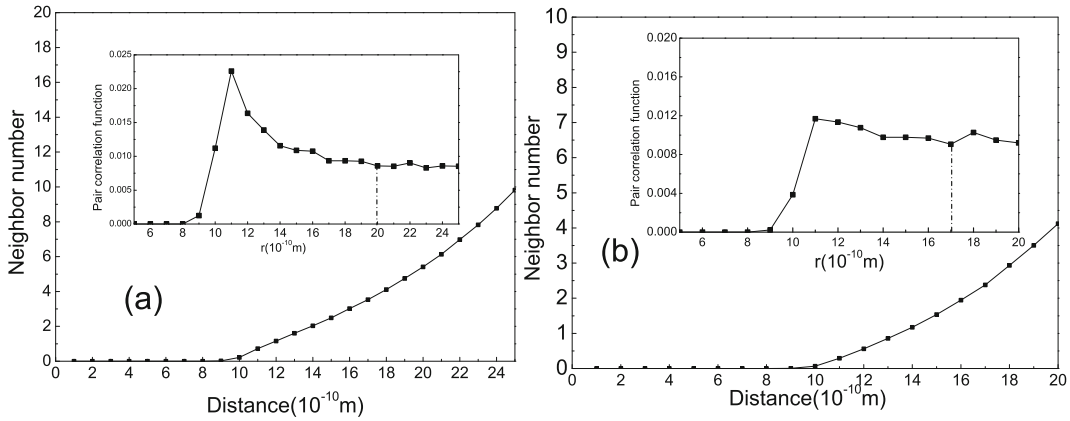

Fig. 5. Neighbor number distribution for protein-counterion before adsorption. (a) Electroneutral with positive and negative surface patches. (b) Electroneutral, with randomly distributed charges.

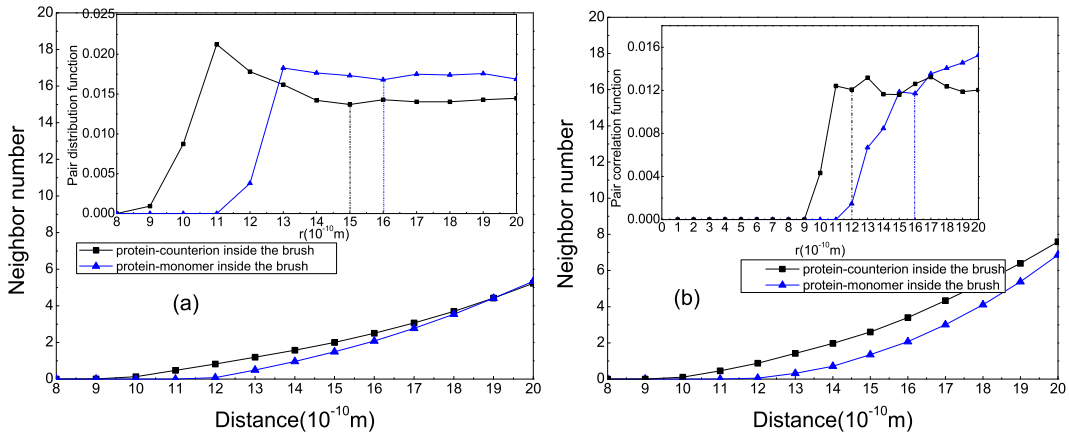

Fig. 6. Neighbor number distributions for protein-monomer and protein-counterion after adsorption. (a) Electroneutral with positive and negative surface patches. (b) Electroneutral, with randomly distributed charges.

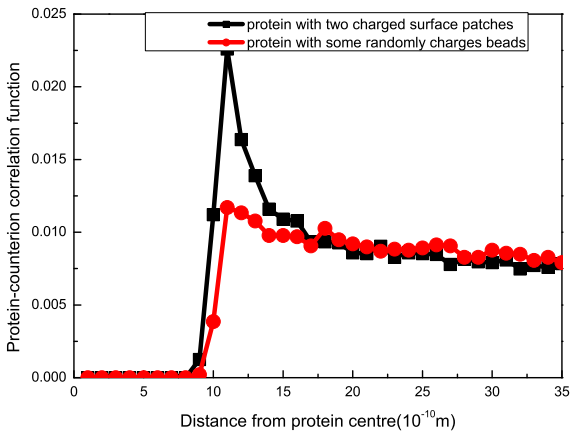

Fig. 7. Protein-counterion correlation function.

Note that any effects of varying pH values are excluded in our simulations. Yet, the adsorption on the wrong side occurs, which supports the assumption that the mechanism of counterion release is sufficiently effective to facilitate the protein adsorption. That does not exclude the possibility of pH effects being the driving force of the observed protein adsorption in some of the experimental setups. The data presented in this paper are not yet sufficiently quantitative to allow for an accurate computation of the free energies of the systems, prior and after protein adsorption, but large scale numerical simulations seem feasible in the future to complete our knowledge about these phenomena. Although the calculation of the free energy is not feasible based on the current data, we can calculate the Coulombic energy change upon adsorption which was taken directly from Coulombic pairwise energy in the simulation. The Coulombic energy based on the protein model used in fig. 4a are -1587 kcal/mol to -1617 kcal/mol separately for prior and after adsorption. It seems that Coulombic interaction does not favor adsorption strongly. Therefore, to a certain extent, it is proving that entropy dominates the adsorption mechanism.

The addition of salt to the system shown in fig. 4(a) results to density distributions as shown in fig. 4(f). A smaller number of proteins is adsorbed in the latter case. Note that the salt concentration, $c_s = 0.03$ M/L, is still smaller than the counterion concentration (inside the brush), and the Debye length, $\lambda_D = 10$ Å, is larger than

the monomer size. These two parameters define that the polyelectrolyte brush has not yet entered its salted brush regime. The salt concentration is sufficiently high to release a considerable amount of adsorbed proteins, a phenomenon that has been found before in experiments [12]. When a finite concentration of salt is added to the system, counterions are released from the brush and from the free proteins as a result of Debye screening. Once the ionic strength is sufficiently high, the system approaches its neutral charge limit in which steric repulsion prevails, so that the proteins do not adsorb anymore.

4 Conclusions

In summary, we have presented simulations for the interaction of fullerene-like inhomogeneously charged proteins with a layer of densely grafted polyelecrolytes. The simulations are able to reproduce the experimental observation that proteins can be adsorbed on polyelectrolyte brushes even on the "wrong side" and that the polyelectrolyte-mediated protein adsorption leads to strong adsorption if the protein has two unlike-charged patches at low ionic strength. These results can be understood with the model of an entropic driving force due to the release of counterions, that are localized about the charge patches of the free proteins, and are released once these proteins enter the brush. Simulations with an alternative protein model with randomly distributed charges, which do not show any counterion condensation, support the claim that counterion release is an important driving force for the protein adsorption. A significantly reduced adsorption takes place at high salt concentrations, so that once adsorbed proteins can be released by the addition of salt to the system.

This work was supported by the national science foundation of China under grant No. 11274258. JUS a cknowledges support from the Marie Curie Initial Training Network "SOMATAI".

References

1. W. Senaratne, L. Andruzzi, C.K. Ober, Biomacromolecule **6**, 2427 (2005).
2. C. Xue, N. Yonet-Tanyeri, N. Brouette, M. Sferrazza, P.V. Braun, D.E. Leckband, Langmuir **27**, 8810 (2011).
3. S. Burkert, E. Bittrich, M. Kuntzsch, M. Muller, K.-J. Eichhorn, C. Bellmann, P. Uhlmann, M. Stamm, Langmuir **26**, 1786 (2010).
4. A. Wittemann, B. Haupt, M. Ballauff, Phys. Chem. Chem. Phys. **5**, 1671 (2003).
5. E. Bittrich, P. Uhlmann, K.-J. Eichhorn, K. Hinrichs, D. Aulich, A. Furchner, in *Ellipsometry of Functional Organic Surfaces and Films*, edited by K. Hinrichs, K.-J. Eichhorn, Vol. **52** of *Springer Series in Surface Sciences* (Springer, Berlin, Heidelberg, 2014) pp. 79–105, ISBN 978-3-642-40127-5.
6. P. Uhlmann, N. Houbenov, N. Brenner, K. Grundke, S. Burkert, M. Stamm, Langmuir **23**, 57 (2007) pMID: 17190485.
7. P.M. Biesheuvel, F.A.M. Leermakers, M.A.C. Stuart, Phys. Rev. E **73**, 011802 (2006).
8. C. Czeslik, R. Jansen, M. Ballauff, A. Wittemann, Phys. Rev. E **69**, 021401 (2004).
9. S. Rosenfeldt, A. Wittemann, M. Ballauff, E. Breininger, J. Bolze, M. Dingenouts, Phys. Rev. E **70**, 061403 (2004).
10. W.M. de Vos, F.A.M. Leermakers, A. de Keizer, M.A. Cohen Stuart, J.M. Kleijn, Langmuir **26**, 249 (2010).
11. A. Wittemann, B. Haupt, M. Ballauff, Prog. Colloid Polym. Sci. **133**, 58 (2006).
12. O. Hollmann, C. Czeslik, Langmuir **22**, 3300 (2006).
13. C. Fleck, H.H. von Grünberg, Phys. Rev. E **63**, 61 (1990).
14. M. Delcroix, S. Laurent, G. Huet, C. Dupont-Gillain, Acta Biomater **11**, 68 (2015).
15. K. Kremer, J. Chem. Phys. **92**, 5057 (1990).
16. R. Hockney, J. Eastwood, *Computer Simulation Using Particles* (McGraw-Hill Inc., US, 1981).
17. D. Frenkel, B. Smit, *Understanding Molecular Simulations* (Academic Press, 2001).
18. E.L. Pollock, J. Glosli, Comput. Phys. Commun. **95**, 93 (1996).